The impact of pressure on NOx formation in a microwave air plasma reactor

A.Hughes [1,2], O. Biondo [1,3], A. Van de Steeg [1], X. Tu [2], G. Van Rooij [1,4]

[1] *Dutch Institute For Fundamental Energy Research, Eindhoven, The Netherlands*
[2] *Department of Electrical Engineering and Electronics, University of Liverpool, Liverpool, L69 3GJ, United Kingdom*
[3] *Research group PLSAMANT, Department of Chemistry, University of Antwerp, Antwerp, Belgium*
[4] *Faculty of Science and Engineering, Maastricht University, Maastricht, The Netherlands*

Abstract: Microwave plasma offer an alternative path to traditional nitrogen fixation, a key process on which a significant amount of the global population owes their lives. Using air as a feedstock removes the dependence on natural gas and allows the coupling of this process with intermittent renewable energy sources. This work will explore the intricate relationship between pressure and the performance of sub-atmospheric air plasma for nitrogen fixation.

Keywords: Air plasma, Nitrogen fixation, Microwave plasma

1. Introduction

In a push towards a global net zero, all industries must access ways in which they can reduce their CO_2 emissions. Currently, one of the most produced chemicals in the world is NH_3, which is a critical component of N_2-based Fertilisers, which is produced by the Haber-Bosch (HB) process, which the is shown by Eq. 1.

$$N_2 + 3H_2 \rightarrow 2NH_3 \qquad \text{Eq. 1}$$

Typically, H_2 is obtained from steam reforming of natural gas, producing CO_2 as a waste product. The application of plasma provides an opportunity to use air as a feedstock for nitrogen fixation to produce NO_x, which can then be converted into nitric acid (HNO_3). The HB process has been refined and is now approaching its theoretical energy efficiency limit. Theoretically, non-thermal air plasma provides an alternative path with a minimum energy cost of approximately 0.2 MJ mol^{-1} [1]. Thermal formation of NO_x through the Zeldovich mechanism, as described in Eqs. 2 and 3, has been studied since at least the 1950s.

$$N_2 + O \rightarrow NO + N \qquad \text{Eq. 2}$$
$$N + O_2 \rightarrow NO + O \qquad \text{Eq. 3}$$

Plasma provides an alternative path through the so-called vibration Zeldovich mechanism shown in Eqs. 4 and 5 [2].

$$N_2(v > 12) + O \rightarrow NO + N \qquad \text{Eq. 4}$$
$$NO + O \rightarrow NO_2 \qquad \text{Eq. 5}$$

This study explores the dependence of reactor performance on pressure using *in-situ* rotational Raman and *ex-situ* FTIR. The N≡N bond is one of the strongest molecular bonds and thus significant energy is required to break it. Microwave plasmas have high gas temperatures (T_g) allowing for the dissociation of N_2 thus allowing the formation of NO_x species. Understanding how reactor conditions can be tailored to maximize production without excess energy being wasted as heat is key to the proliferation of this technology.

2. Experimental

The plasma is generated using continuous 2.45 GHz microwaves (MW), inside a 30mm (27mm inner diameter) quartz tube. The gas is fed into the reactor tangentially at the opposite end of the reactor to which the effluent leaves, creating a forward vortex. More details on the MW reactor details can be found in [3].

The in-situ measurements presented in this work are taken using a 532 nm frequency-doubled Nd:YAG (30 Hz, 400mJ per pulse) Spectra Physics GCR-230 laser, which is focused in the center of the waveguide. The scattered light is collected by the fiber optic array and transmitted to the custom-built Littrow spectrometer via an optical cable. The system is calibrated using the same method as previous work by our group [4], [5]. The sensitivity of the majority of the optical equipment used in this work has been corrected using an integrating sphere. The effluent of the

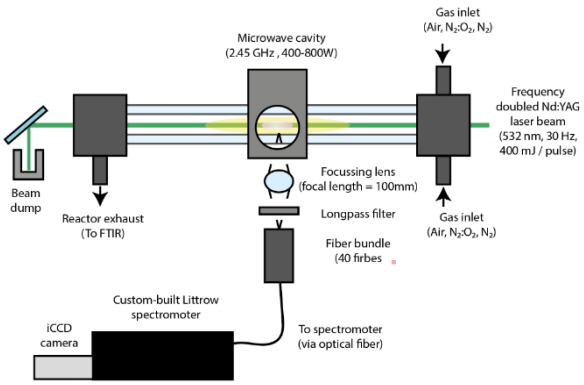

Figure 1 - Schematic diagram of the sub-atmospheric plasma setup at DIFFER

reactor is fed into an in-line FTIR, which is used for the effluent characterization. A schematic diagram of the experimental setup is shown in Figure 1.

3. Results and Discussion

The performance data for the microwave plasma reactor is shown in Figure 2. It can be seen from Figure 2 that there is a decrease in reactor performance with increasing pressure; this naturally leads to a reduction in energy efficiency. Considering the vibrational Zeldovich mechanism, this reduction in reactor performance is expected to occur with increasing pressure due to an increase in gas heating, promoting Vibration-Translation (V-T) relaxation over Vibration-Vibration (V-V) relaxation. Despite this, similar reactors found in the literature operating at atmospheric pressure have achieved noticeably higher performance [6]. This implies another mechanism is at play that causes these changes in reactor performance.

The T_g and O_2 dissociation fraction of the air plasma in the center of the tube and waveguide are presented in Figure 3a and 3b, respectively. The T_g for 400 mbar is much higher than that of 80 mbar and drops much more quickly, which is indicative of a contraction of the plasma. The O_2 dissociation fraction of the plasma follows much the same trend, due to the dominant role of thermal chemistry over plasma chemistry.

The temperature measurements are used to calculate the expected thermodynamic mole fraction of the different species inside the plasma using Cantera [7], the results of which are shown in Figure 4. The dashed line represents the measured T_g for the respective condition. As can be seen in Figure 4, at 80 mbar, the dashed line is within the temperature range at which NO formation is favorable, where as at 400 mbar the T_g is above this range and is high enough to result in significant thermal dissociation of N_2 into N atoms. N atoms have been demonstrated to be one of the primary loss mechanisms of NO [8]. The combination of these two factors explains the reduction in performance at 400 mbar.

As the reactor pressure increases from 80 to 400 mbar the gas temperature increases from ≈4500 to ≈6400 K. The maximum thermal equilibrium mole fraction for NO increase more slowly from ≈2800-3200 K to 3100-3500 K (80 and 400 mbar, respectively). As pressure increases further, the maximum NO formed continues to increase, so does the temperature at which this maxima occurs, but the

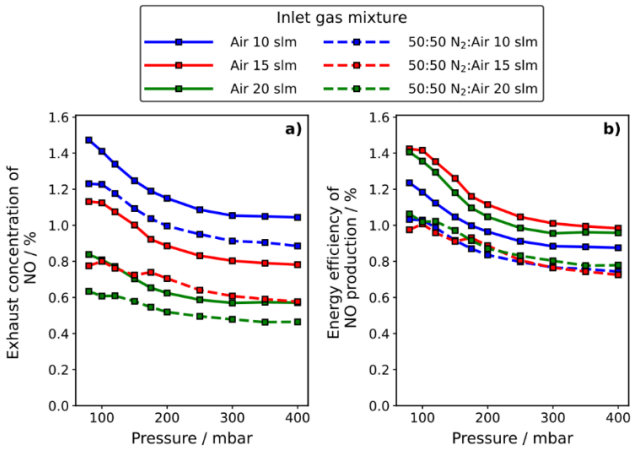

Figure 2 - Performance data for air plasma reactor at 800 W. a) shows the exhaust concentration on NO, b) the energy efficiency of NO formation. The dashed lines represent a dilution of air with N_2 reducing the oxygen concentration from approximately 20% to approximately 10%.

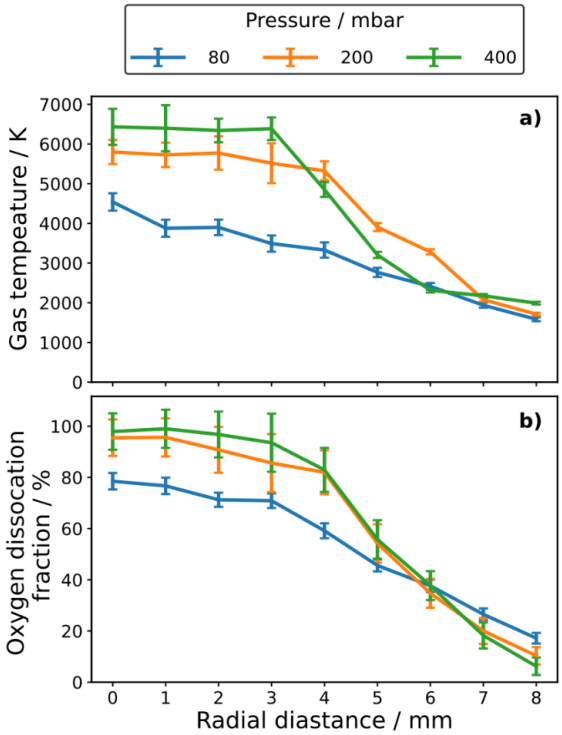

Figure 3 – rotational Raman measurements were taken at different pressures for air plasma 10slm 800w showing a) the gas temperature and b) the oxygen dissociation fraction.

gas temperature inside the reactor does not increase significantly. This means that as pressure increases past 400 mbar there will arrive a point at which the T_g and thermodynamically optimal conditions are once again aligned, thus improving the reactor performance to levels above 80 mbar.

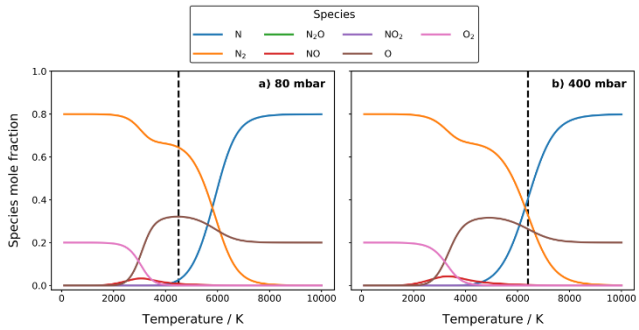

Figure 4 – Species mole fraction of air (80% N2: 20% O2) with respect to temperature for a) 80mbar and b) 400 mbar calculated using Cantera. The dotted line represents the T_g measured in the center of the reactor using rotational Raman.

4. References

[1] V. D. Rusanov, A. A. Fridman, and G. V. Sholin, "The physics of a chemically active plasma with nonequilibrium vibrational excitation of molecules," 1981.

[2] B. Gordiets and A. Ricard, "Production of N, O and NO in N_2 -O_2 flowing discharges," *Plasma Sources Sci. Technol.*, vol. 2, no. 3, pp. 158–163, Aug. 1993, doi: 10.1088/0963-0252/2/3/005.

[3] N. Gatti *et al.*, "Preferential vibrational excitation in microwave nitrogen plasma assessed by Raman scattering," *Plasma Sources Sci. Technol.*, vol. 27, no. 5, p. 055006, May 2018, doi: 10.1088/1361-6595/aabd60.

[4] T. Butterworth *et al.*, "Plasma induced vibrational excitation of CH_4 —a window to its mode selective processing," *Plasma Sources Sci. Technol.*, vol. 29, no. 9, p. 095007, Sep. 2020, doi: 10.1088/1361-6595/aba1c9.

[5] D. C. M. van den Bekerom, A. van de Steeg, M. C. M. van de Sanden, and G. J. van Rooij, "Mode resolved heating dynamics in pulsed microwave CO_2 plasma from laser Raman scattering," *J. Phys. D: Appl. Phys.*, vol. 53, no. 5, p. 054002, Jan. 2020, doi: 10.1088/1361-6463/ab5311.

[6] S. Kelly and A. Bogaerts, "Nitrogen fixation in an electrode-free microwave plasma," *Joule*, vol. 5, no. 11, pp. 3006–3030, Nov. 2021, doi: 10.1016/j.joule.2021.09.009.

[7] "David G. Goodwin, Harry K. Moffat, Ingmar Schoegl, Raymond L. Speth, and Bryan W. Weber. Cantera: An object-oriented software toolkit for chemical kinetics, thermodynamics, and transport processes."

[8] O. S. Bahnamiri, C. Verheyen, R. Snyders, A. Bogaerts, and N. Britun, "Nitrogen fixation in pulsed microwave discharge studied by infrared absorption combined with modelling," *Plasma Sources Sci. Technol.*, vol. 30, no. 6, p. 065007, Jun. 2021, doi: 10.1088/1361-6595/abff0e.